Electronic Supplementary Material (ESI) for RSC Advances.

Supporting Information for:

Revealing the Explosives-Detection Mechanism of a Luminescent Zinc MOF: the Roles of Hydrogen Bond and π–π Stacking

Lei Liu[a,b], Juanyuan Hao[a], Yantao Shi[a], Jieshan Qiu[a], and Ce Hao*[a]

Correspondence to: Ce Hao (E-mail: *haoce@dlut.edu.cn*)

[a]Lei Liu, Juanyuan Hao, Yantao Shi, Jieshan Qiu, Ce Hao

State Key Laboratory of Fine Chemicals, Dalian University of Technology, Dalian 116024, China

[b]Lei Liu

State Key Laboratory of Molecular Reaction Dynamics, Dalian Institute of Chemical Physics, Chinese Academy of Sciences, Dalian 116023, China

The authors declare no competing financial interest.

Page Contents:

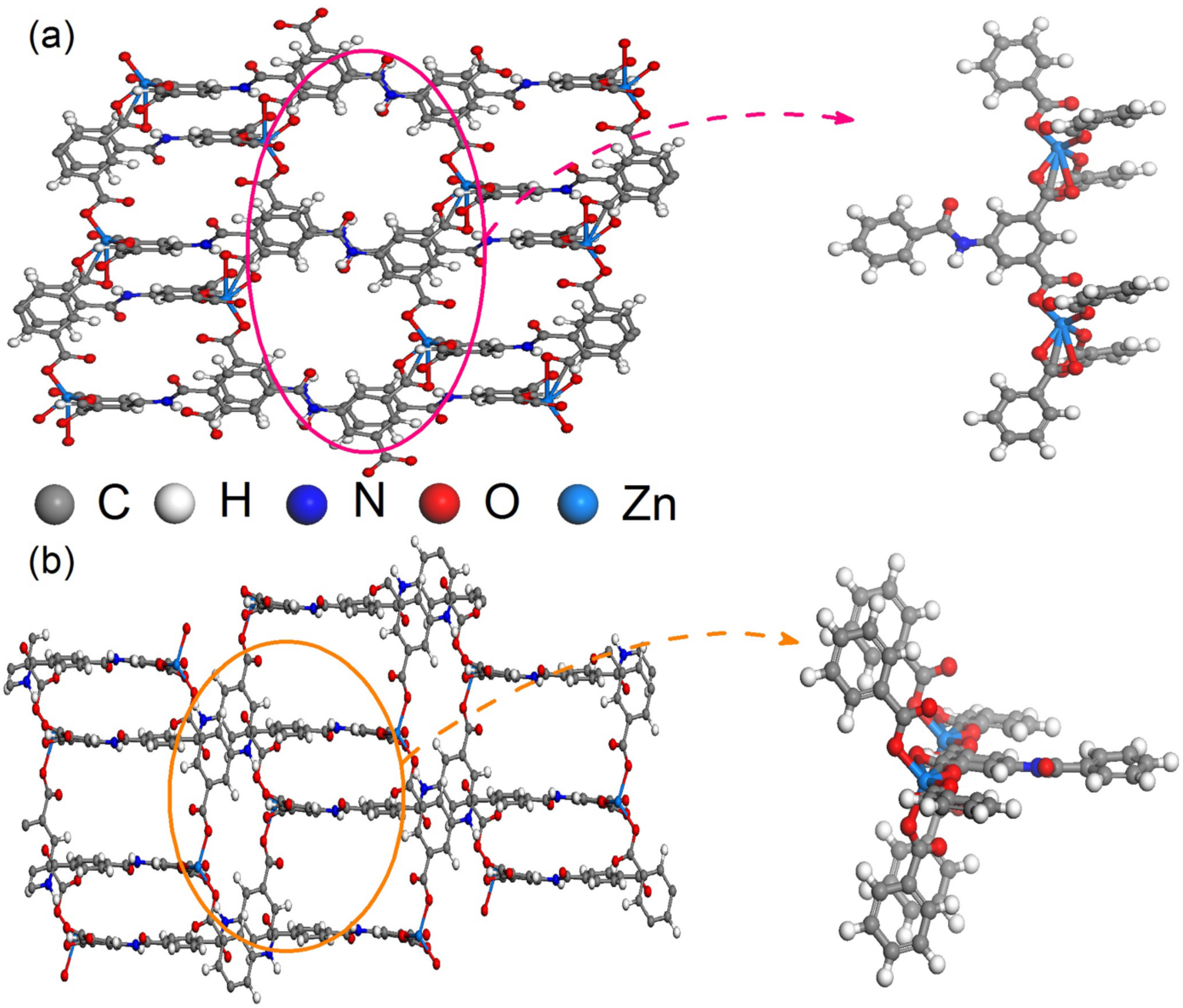

Figure S1. Truncating of the cluster models from different perspectives. (a) Top view; (b) side view.

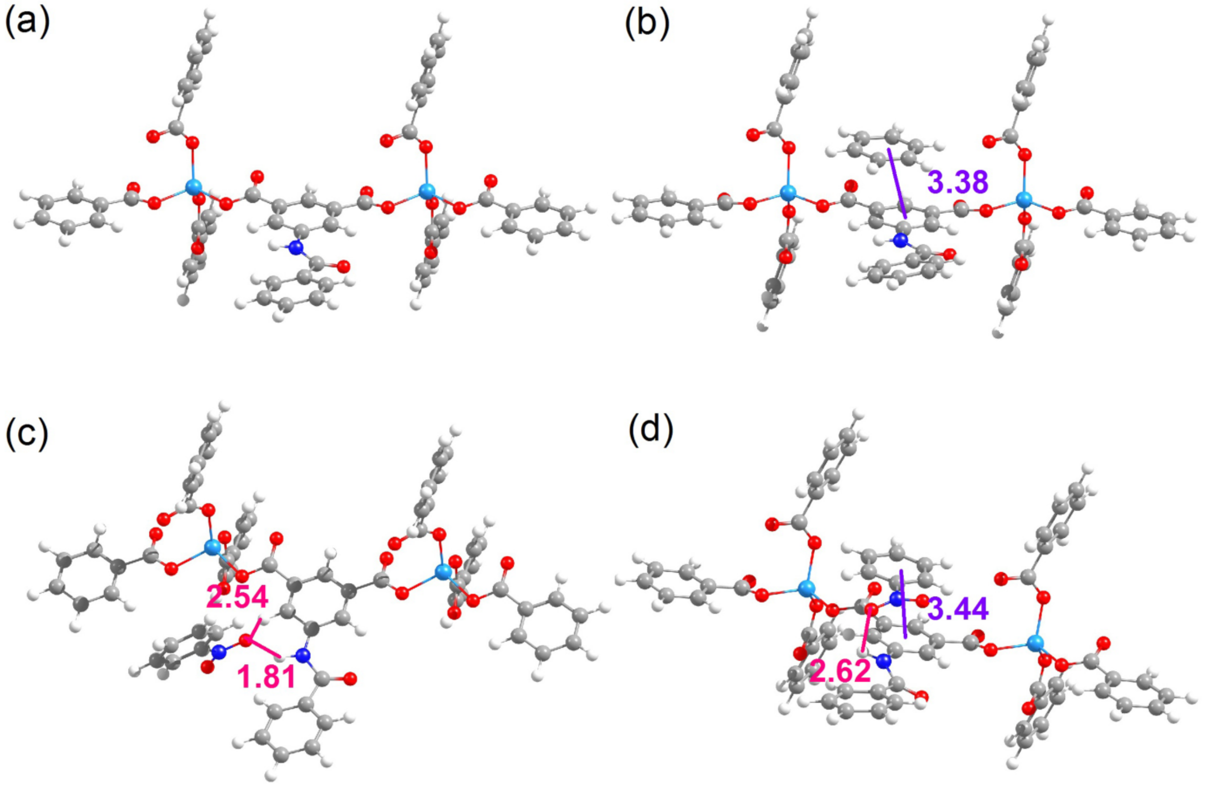

Figure S2. Cluster models for (a) LMOF 1, (b) Ben-MOF, (c) NB1-MOF and (d) NB2-MOF. Hydrogen bond lengths are given in red fonts and centroid distances between aromatic rings are given in purple fonts.

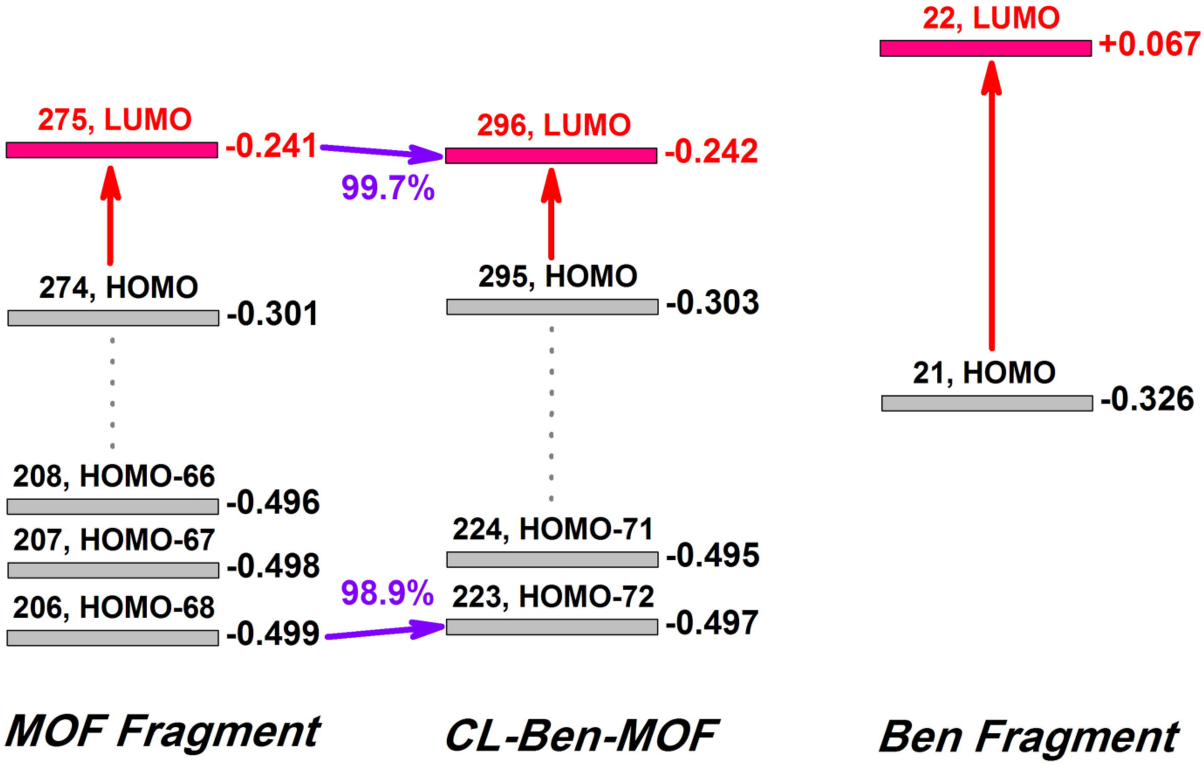

Figure S3. Detailed fragment orbital interaction diagram for CL-Ben-MOF. Contributions of the fragment orbitals to corresponding complex orbitals are given around the purple arrows. Energy values (Hartree) for each orbital are listed beside the corresponding orbitals.

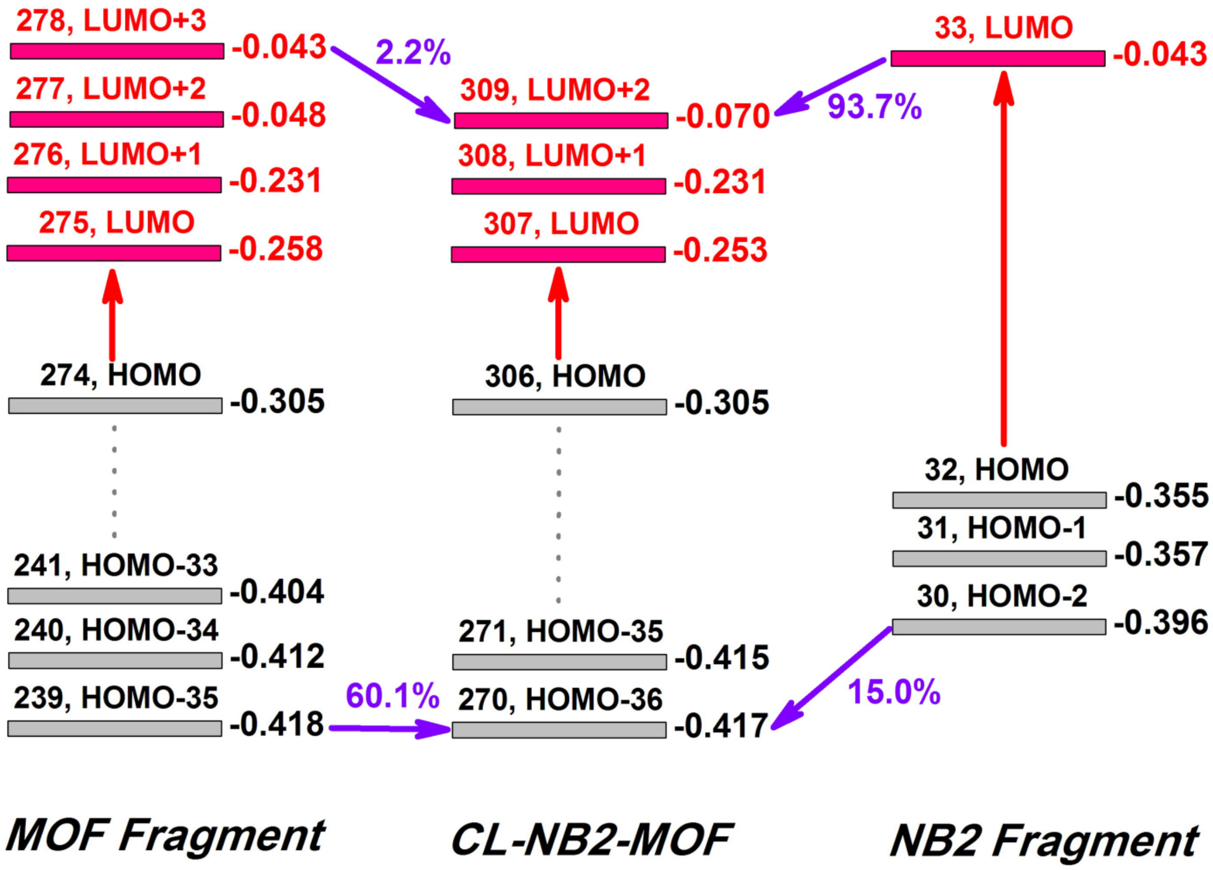

Figure S4. Detailed fragment orbital interaction diagram for CL-NB2-MOF. Contributions of the fragment orbitals to corresponding complex orbitals are given around the purple arrows. Energy values (Hartree) for each orbit are listed beside the corresponding orbitals.

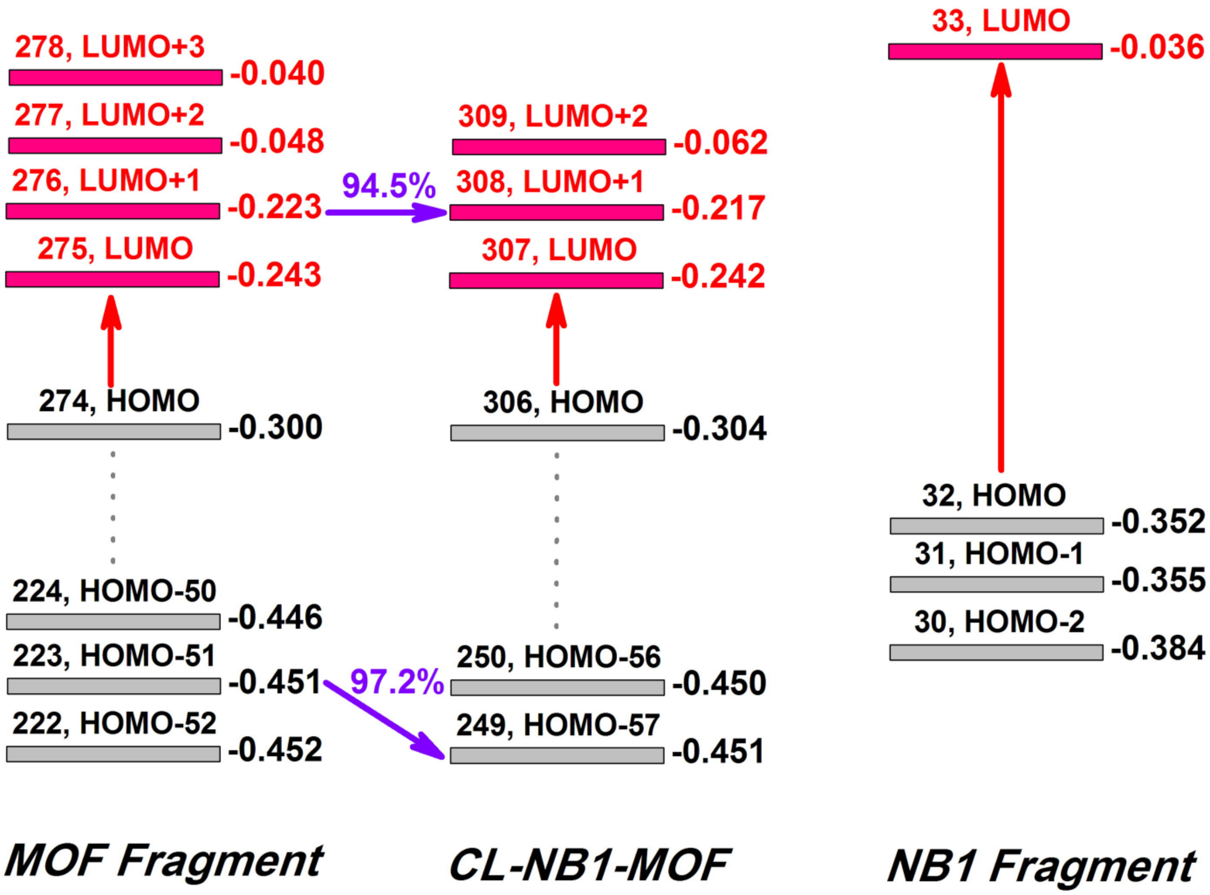

Figure S5. Detailed fragment orbital interaction diagram for CL-NB1-MOF. Contributions of the fragment orbitals to corresponding complex orbitals are given around the purple arrows. Energy values (Hartree) for each orbit are listed beside the corresponding orbitals.

Table S1. Calculated lattice parameters and corresponding experimental data. Deviations from experimental data are shown in parentheses.

Lattice Parameter	CASTEP/PBE	CASTEP/PW91	expt[a]
a (Å)	10.3 (3.0%)	10.3 (3.0%)	10.0
b (Å)	10.5 (1.9%)	10.5 (1.9%)	10.3
c (Å)	18.5 (3.3%)	18.5 (3.3%)	17.9
α (degrees)	105.0 (1.2%)	104.9 (1.2%)	103.7
β (degrees)	104.3 (4.7%)	104.2 (4.7%)	99.6
γ (degrees)	90.8 (2.8%)	90.9 (2.8%)	93.4

[a] Experimental data obtained from reference 44.

Optimizations of the Crystal Structures: The crystal structure for LMOF 1 is optimized using the experimentally determined single-crystal X-ray diffraction structure as the starting geometry.[44] Two different theoretical methods are used to generate the unit cell structures and compared with experimental data to test the credibility of our calculation results (namely CASTEP/PBE, and CASTEP/PW91). As reported in Table S1, all the calculated lattice parameters are within an error of 5% compared to the experimental data. These errors may originate from the fact that the calculations are performed at 0K in vacuum while the experiment results are obtained at room temperature. Anyway, all the errors are among the acceptable region considering the complexity of the MOF structure which would have negligible effect on the results of our research. Besides, the fact that the two different theoretical approaches predict nearly identical crystal structures gives us further confidence in the reliability of the theory.

Table S2. Calculated lattice parameters with different k-point settings.

	1×1×1	2×1×1	2×2×1	2×2×2
α (degrees)	104.97944	104.97407	104.96067	104.95898
β (degrees)	104.29786	104.29241	104.29268	104.29316
γ (degrees)	90.84302	90.8453	90.85576	90.85721
a (Å)	10.321824	10.311384	10.315169	10.315322
b (Å)	10.552241	10.542823	10.530567	10.529766
c (Å)	18.518689	18.514765	18.516593	18.517734

k-Piont Testing. The effect of the k-points on the optimization of the crystal structure have been tested and listed in Table S2. Using the optimized geometry with the Γ-point, we reoptimized the unitcell with the k-point grid of 2 × 1 × 1, 2 × 2 × 1, and 2 × 2 × 2, respectively. As shown in the table, the k-points seem to have little effect on the unitcell parameter. Besides, we are dealing with a large system (184 atoms per unitcell), the Gamma point alone is sufficient for the optimization of the crystal structure.

Table S3. Calculated absolute energies and the corresponding binding energies for the three adsorbates.[a]

Structure	Analyte	Framework	Total Energy	Binding energy
Ben-MOF	-1026.170792190	-42114.92946607	-43141.86436866	0.7641104
NB1-MOF	-2151.212478121	-42114.81412550	-44267.02138081	0.994777*2*
NB2-MOF	-2151.213167652	-42114.93184739	-44267.10410654	0.959091*5*

[a] The binding energies are abtained by using the following equation: $E_{interaction}=E_{LMOF}+E_{analyte}-E_{LMOF+analyte}$, All the energies are given in electron volt (eV).

Table S4. Selected calculated electronic transition energies, corresponding oscillator strengths (f), orbital contributions (contrib), compositions (comp) and transition characters (character) of the singlet excited states of the four clusters.[a]

Cluster	Transition	abs. (nm/eV)	f	contrib	comp	character
CL-LMOF **1**	$S_0 \rightarrow S_{98}$	321.8/3.85	0.0000	H-38→L+1	61.2%	LLCT, ILCT
	$S_0 \rightarrow S_{99}$	321.2/3.86	0.0577	H-71→L	78.1%	LLCT, ILCT
	$S_0 \rightarrow S_{100}$	317.8/3.90	0.0002	H-54→L	36.9%	LLCT, ILCT
CL-Ben-MOF	$S_0 \rightarrow S_{94}$	330.2/3.75	0.0000	H-38→L+1	39.9%	LLCT, ILCT
	$S_0 \rightarrow S_{95}$	324.9/3.82	0.0350	H-72→L	71.1%	LLCT, ILCT
	$S_0 \rightarrow S_{96}$	323.1/3.84	0.0047	H-57→L	66.7%	LLCT, ILCT
CL-NB1-MOF	$S_0 \rightarrow S_{95}$	350.2/3.54	0.0000	H-39→L	96.8%	LLCT
	$S_0 \rightarrow S_{96}$	344.7/3.60	0.0094	H-57→L+1	87.0%	LLCT
	$S_0 \rightarrow S_{97}$	341.6/3.63	0.0037	H-56→L	67.7%	LLCT
CL-NB2-MOF	$S_0 \rightarrow S_{101}$	340.1/3.65	0.0048	H-57→L	81.6%	LLCT, ILCT
	$S_0 \rightarrow S_{102}$	338.4/3.66	0.0130	H-36→L+2	29.3%	MOF→analyte
	$S_0 \rightarrow S_{103}$	338.3/3.66	0.0000	H-40→L	80.6%	LLCT, ILCT

[a] LLCT represents ligand to ligand charge transfer, ILCT represents intra-ligand charge transfer, “MOF→Analyte” represents electron transfer from MOF to analyte molecule.

Selection of Molecular Orbitals. The selection of molecular orbitals involved in the excitation processes are based on the following motivations and in order to make the explanation clear, CL-NB2-MOF has been taken as the example.

1. First, the excited states involved in the electronic transition are confirmed by analyzing the excitation process. As shown in Table S4, the electronic transition corresponding to the excitation around 330nm in the experiment should be the $S_0 \rightarrow S_{102}$ transition which has the largest oscillator strength. Indeed, the excitation energies of the $S_0 \rightarrow S_{101}$ and $S_0 \rightarrow S_{103}$ transitions are close to that of the $S_0 \rightarrow S_{102}$ transition. However, the oscillator strength is significantly different. Based on this, $S_0 \rightarrow S_{102}$ transition should represent the real case electronic transition and is chosen for further study.
2. Then the composition of the $S_0 \rightarrow S_{102}$ transition is analyzed. We find that the largest composition of the $S_0 \rightarrow S_{102}$ transition corresponds to the HOMO-36→LUMO+2. The two molecular orbitals (H-36, L+2) involved in the excitation process is thus confirmed.
3. Finally, compositions of the molecular orbital H-36 (270) and L+2 (309) are analyzed. As shown in the figure below (also in Figure S4, Supporting Information), 270 are composed from two fragment orbitals namely 239 fragment orbital from fragment MOF and 30 fragment orbital from fragment nitrobenzene. Although fragment orbital 240 is close in energy to fragment orbital 239, it does not contribute to the molecular orbital involved in the excitation process. Based on this, orbital 240, which is close in energy to 239, is not concerned. For the case of molecular orbital 309, only fragment orbital 278 from fragment MOF contributes to this molecular orbital. Fragment orbital 277, which is close in energy to 278, is excluded. In conclusion, fragment orbitals 239, 278 from MOF fragment and fragment orbitals 30, 33 from nitrobenzene fragment are chosen in defining the interaction mechanisms.
4. This selection procedure is applied in the analyses of other clusters namely CL-Ben-MOF and CL-NB1-MOF.